Received Date:29th November, 2025
Revision Date: 15th December, 2025
Accepted Date: 5th February, 2026

Design and Empirical Validation of a Mid-Range Wireless Power Transfer System Using Magnetic Resonance Coupling

Anveshan Timsina[1*], Sandesh Dhital[2], Saroj Nagarkoti[3], Utsab Dahal[4], Kobid Karkee[5]

[1]Dept. of Electronics and Computer Engineering, Thapathali Campus, Nepal. Email: anveshan.078bei005@tcioe.edu.np
[2] Dept. of Electronics and Computer Engineering, Thapathali Campus, Nepal. Email: sandesh.078bei034@tcioe.edu.np
[3] Dept. of Electronics and Computer Engineering, Thapathali Campus, Nepal. Email: saroj.078bei039@tcioe.edu.np
[4] Dept. of Electronics and Computer Engineering, Thapathali Campus, Nepal. Email: utsab.078bei046@tcioe.edu.np
[5]Asst, Prof, Dept. of Electronics and Computer Engineering, Thapathali Campus, Nepal. Email: karkeekobid009@gmail.com

Abstract— Conventional inductive power transfer is fundamentally limited by the rapid decay of magnetic flux density, restricting efficient energy transmission to near-contact distances. This research addresses this spatial limitation through the design, simulation, and empirical validation of a mid-range wireless power transfer system based on magnetic resonance coupling. The system employs a Class-B push-pull power amplifier driving high-quality factor helical coils with a diameter of 30 centimeters and 6 turns, tuned to a nominal resonant frequency of 1 megahertz. Through integrated finite element method magnetostatic simulations and circuit analysis, the system was optimized to maximize flux linkage while minimizing skin effect losses. Experimental validation demonstrated that the magnetic resonance coupling topology significantly extends transmission range compared to non-resonant inductive coupling. At a separation of 20 centimeters, the resonant system delivered 5.4 volts to the load, whereas the inductive baseline achieved only 0.33 volts. The system achieved a peak end-to-end efficiency of 19.01 percent and maintained functional power transfer up to 40 centimeters. These findings confirm that resonant impedance matching provides a scalable pathway for mid-range charging applications when frequency tracking mechanisms compensate for dynamic coupling variations.

Keywords — Magnetic Resonance Coupling, Wireless Power Transfer, Helical Coils, Resonance, Class-B Power Amplifier

I. Introduction

The concept of transferring electrical energy without physical interconnects has intrigued the scientific community for over a century. Nikola Tesla is recognized as the pioneer of this domain, primarily through his development of the "Apparatus for Transmitting Electrical Energy," also known as the Wardenclyffe Tower, in the early 20th century [1]. Although Tesla's facility was never fully operational due to funding constraints, his work established the foundational theories of the field. Decades later, the advent of microwave technology revitalized the potential for wireless energy transmission, a prospect that had largely stagnated following Tesla's initial endeavors [2]. In the contemporary era, Wireless Power Transfer (WPT) is classified into two primary categories: Radiative (e.g., Directive RF Beamforming) and Non-Radiative. Additionally, a third category utilizing Acoustic or Ultrasonic Reverberation is currently being explored, though it remains in the preliminary stages of development [3]. Non-Radiative methods, which are the focus of consumer electronics, encompass Inductive Coupling, Magnetic Resonance Coupling, and Capacitive Coupling [4].

Despite the commercial availability of wireless charging, the predominant technology relies on electromagnetic induction, which necessitates precise alignment and direct physical contact between the receiving device and the charging pad. In a society characterized by the ubiquity of battery-dependent electronic devices, this contact-based paradigm fails to address the ergonomic requirements for seamless mobility. The reliance on physical docks introduces logistical inefficiencies and "range anxiety," creating a distinct technical demand for a system capable of delivering energy across a significant air gap without physical tethers.

This paper presents the design and implementation of a WPT system utilizing Magnetic Resonance Coupling (MRC) to achieve mid-range power transfer. Unlike standard inductive coupling, which is limited to short-range interaction, MRC employs tuned resonant frequencies to facilitate energy exchange between non-contact coils. The primary objective is to develop a system operating in the MHz frequency

* *Corresponding Author*

range, capable of transferring a minimum of 0.5W over a distance of approximately 30 centimeters. This specification is sufficient to power low-energy electronics such as microcontroller boards, smartwatches, and fitness trackers.

The scope of this research encompasses the fabrication of a transmitter and receiver pair to serve as a proof-of-concept for mid-range consumer electronics charging. While the system demonstrates the potential for spatial freedom in power delivery, it is subject to physical limitations, specifically the inverse relationship between transmission distance and power efficiency. Beyond the optimal range, efficiency declines, rendering the system unsuitable for high-power applications. Nevertheless, this study reinforces the viability of resonant coupling as a solution for contactless energy distribution, offering a pathway toward a charging ecosystem where devices maintain operation without active user intervention.

II. Related Work

The theoretical foundation of Wireless Power Transfer (WPT) was established in the 19th century through the formulation of fundamental electromagnetic principles, including Ampere's law, Biot-Savart's law, Faraday's law, and Maxwell's equations. While early experimental demonstrations were conducted by H.R. Hertz and subsequently expanded upon by Nikola Tesla through his extensive work on microwave-based transmission, the technology remained largely experimental for over a century. Although scientifically validated, widespread commercial viability has historically remained elusive [4, 5].

Contemporary WPT technologies are generally categorized into three distinct modalities based on the transmission mechanism: Radiative (Far-Field), Non-Radiative (Near-Field), and Acoustic (Ultrasonic) [6, 4].

A. *Radiative and Acoustic Methodologies*

Radiative technologies utilize diffused RF or microwave signals (300 MHz to 300 GHz) to transmit energy over long distances. The process typically involves converting DC to RF at the source and rectifying received RF waves back to DC at the load [3].

While this method supports mobility and ranges extending to several kilometers, it faces significant challenges regarding efficiency and safety. For instance, Xiaomi has explored Directive RF Power Beamforming, utilizing a 144-antenna array to deliver up to 5 watts via millimeter waves [7]. However, millimeter-wave technology is susceptible to physical obstruction [8], and the high-power beacons required for such systems raise concerns regarding compliance with FCC and IEEE C95.1-2005 exposure limits [9, 10].

Alternatively, Acoustic or Ultrasonic Reverberation-based systems utilize the piezoelectric effect to transmit energy through air or water. This method offers unique advantages, including resistance to electromagnetic interference and the ability to penetrate solid and liquid media [11]. However, this technology remains in a nascent stage of development [3].

Non-radiative techniques, which rely on near-field magnetic or electric coupling, are currently the most prevalent for consumer electronics.

Inductive Coupling: Inductive Power Transfer (IPT) operates on the principle of magnetic induction, comparable to a standard transformer, where a varying magnetic field in a primary coil induces voltage in a secondary coil [3, 4].

This method is the standard for current commercial applications (e.g., WPC/Qi standards) [13]. While safe and efficient at very close proximity (typically <20cm), IPT suffers from rapid efficiency decay with distance, sensitivity to misalignment, and eddy current losses in metallic environments [6, 14].

Capacitive Coupling: Capacitive coupling utilizes electric fields generated between conductive plates to transfer energy [12]. While this method mitigates some eddy-current losses associated with inductive systems and offers better misalignment tolerance [15], it is generally constrained by low power density and high electric field emissions [6, 16].

Magnetic Resonance Coupling (MRC): MRC utilizes evanescent wave coupling between two resonant coils tuned to the same frequency. Unlike inductive coupling, MRC maintains high efficiency over mid-range distances and is largely immune to non-resonant dielectric obstructions [4, 18]. Consequently, MRC is identified as the most promising method for applications requiring spatial freedom [19].

B. *Experimental Precedents in Magnetic Resonance*

Seminal work by MIT researchers in 2007 demonstrated the efficacy of MRC by powering a 60W bulb at a distance of 2 meters (approximately 8 times the coil radius) with 40% efficiency using 30cm copper coils resonating at 10 MHz [17]. This study confirmed that efficiency remains stable even when line-of-sight is obstructed by dielectric materials.

Subsequent studies have highlighted the trade-offs between coil geometry, frequency, and wire type. In 2015, researchers achieved 85% efficiency at 10cm using 15cm coils [20]. Conversely, a 2016 study demonstrated 20W transfer at 1.1 meters utilizing Litz wire to mitigate skin effect losses, albeit with a lower efficiency of approximately 20% [21]. Further research in 2017 indicated that while lower frequencies (100 kHz) combined with ferrite cores can achieve high efficiency (75%) at short ranges, they are less effective for mid-range transmission compared to MHz-range systems [24].

Recent advancements suggest that coil geometry is a critical optimization parameter [22]. While large helical coils remain the standard for omnidirectional transmission, 2024 research proposes novel square-hexagonal hybrid designs that may offer a 17% improvement in coupling coefficients over traditional geometries [23].

III. Material and methods

A. *Wireless Power transfer*

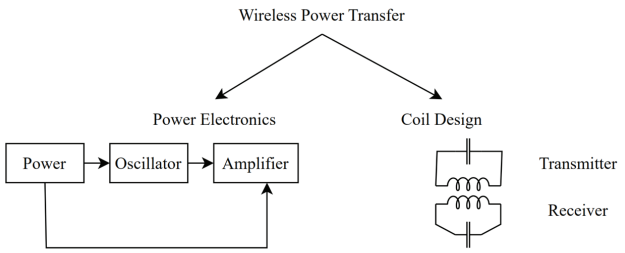

Fig. 1 Phases of wireless power transfer

Any and all wireless transfer systems generally work in two phases: Power Electronics and Coil Design. Power Electronics (oscillators, amplifiers, etc.) is the backbone of any WPT system, governing how electrical energy (or power) is generated, converted, regulated, and delivered to the transmitter coil. Likewise, coil design determines how effectively that energy is transferred. The efficiency and range of power transfer heavily depend on how well the coils are designed as well as on their positioning with respect to each other.

B. *Magnetic Resonance Coupling*

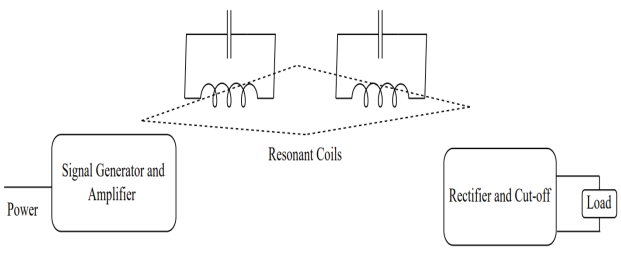

Fig. 2 Magnetic Resonance Coupling

Magnetic Resonance Coupling (MRC) is a non-radiative technique of wireless power transfer based on resonance, in which the energy (or power) is transferred between two objects (coils) through their resonant magnetic fields. It uses a resonant LC circuit, formed by the combination of transmitter coil and a capacitor, to generate a time-varying magnetic field. When the input AC signal matches the resonant frequency, the LC circuit achieves resonance, such that energy oscillates between the inductor (coil) and the capacitor.

The resonant frequency is given by:

$$f_r = \frac{1}{2\pi\sqrt{LC}} \quad (1)$$

Where, f_r = Resonant frequency, L = Inductance, C = Capacitance.

C. *Comparison of MRC and Inductive Coupling*

The coupling factor for inductive coupling (relying on simple inductor-to-inductor coupling) is given by:

$$k = 1.4\left(\frac{R_1R_2}{R_1^2+r^2}\right)^{\frac{3}{2}} \quad (2)$$

Where R_i is the radius of i^{th} coil and r is the distance between their centers. The receiver needs to be very close in effectively order to use non-resonant magnetic coupling however, the coupling can be greatly enhanced by using resonance even when the distance between coils is increased. The power transfer efficiency for a magnetic resonant system is given by:

$$\frac{P_2}{P_1} = \frac{\omega^2M^2R_1R_2}{(R_1R_2)^2} = \frac{\omega^2k^2L_1L_2}{R_1R_2} = k^2Q_1Q_2 \quad (3)$$

This shows that the power transfer depends on the square of the coupling coefficient multiplied by the quality factors of the resonators. The rather fast decay, due to distance between coils, can be mitigated by using additional resonating circuit(s), each of which increase the power transfer ratio by Q times, providing a means for midrange power transfer.

D. *Block Diagram*

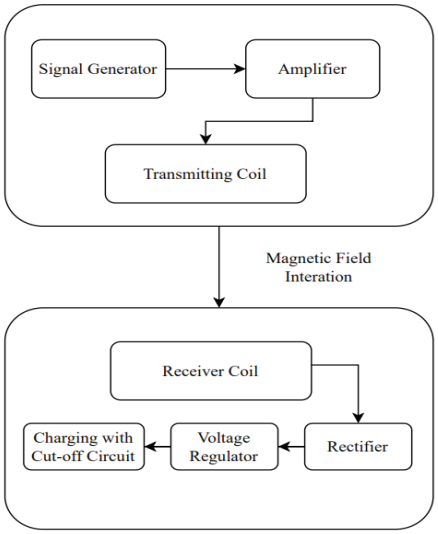

Fig. 3 System Block Diagram

The system begins with an AC power supply that provides the necessary energy for the wireless charging system, typically drawn from a standard AC mains source. The AC power runs a signal generator, which is a special-purpose oscillator capable of producing sine, square, and triangle waveforms and can be used to generate a stable AC signal with desired frequency (calculated resonant frequency). The oscillator's output, generally a low power signal, is sent to a class B amplifier that boosts the signal to the required power level. The output signal from the amplifier is fed to the transmitter coil, which is wound using copper wire for high-frequency operation. The transmitter coil transmits a resonant magnetic field, which extends into the surrounding space and interacts with the receiver coil placed in its vicinity. The receiver coil, connected electrically to the device to be charged (e.g., airpods), captures the magnetic field and induces an AC current in the coil at the same resonance frequency as transmitted. The induced AC current, directly proportional to the strength of the magnetic field, is fed into a rectifier circuit. A smoothing capacitor filters the ripples in the rectified DC to provide a stable output suitable for charging. This smooth DC voltage is then passed through a voltage regulator (e.g., LM7805) to regulate the voltage to the required level and maintain a consistent current flow for efficient battery charging. The system ensures that the device receives suitable voltage and current, and provides auto cutoff along with LED to indicate when charging has stopped.

E. *Transmitter End*

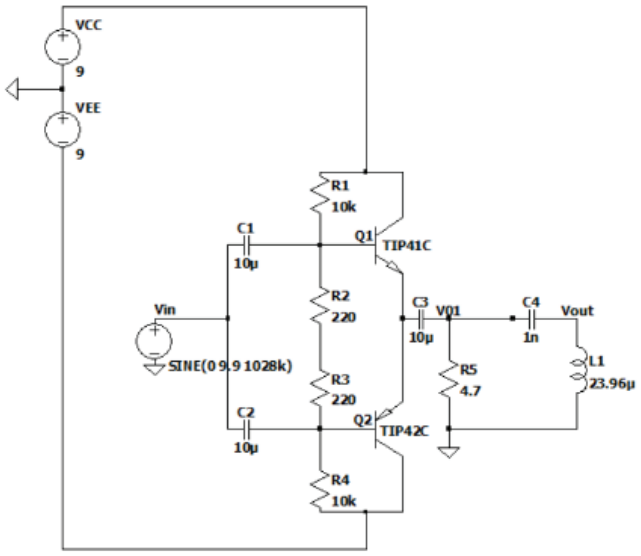

Fig. 4 Transmitter Circuit Diagram

The transmitter circuit design begins with an AC input voltage (say, Vin; not shown in above circuit) which is passed to the function generator which generates a high frequency sinusoidal voltage but with low power. The use of a signal generator allows dynamic changing of the transmission frequency. The capacitors C1 and C2 are used to nullify the dc offset of the sinusoidal signal. The rest of the circuit is a standard Class B Amplifier to amplify the power of the signal given by the signal generator whose output is connected to a resistor R5 in order to draw current. Class B Amplifier consists of a system of two transistors, one NPN (TIP41) and another PNP (TIP42) used in complementary arrangement. They share the output load but handle opposite halves of the input signal cycle. VCC provides the positive voltage to power the transistor, and VEE is used for negative bias purposes i.e., for providing the necessary voltage difference to operate the complementary pair effectively. Then comes the transmitting LC tank. The transmitter coil and capacitor C4 form a series LC tank circuit, which is made to resonate at a specific frequency to generate the alternating magnetic field. This magnetic field is crucial for coupling with the receiver circuit, enabling wireless power transfer.

F. *Receiver End*

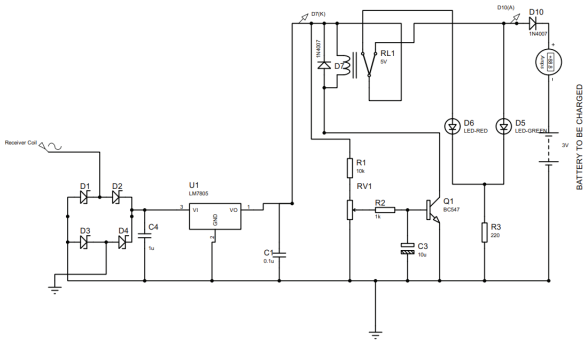

Fig. 5 Receiver Circuit Diagram

This circuit serves as a battery charger with an automatic cutoff mechanism, utilizing a relay to disconnect the battery once it is fully charged. The input AC signal is filtered by the inductor (L1) and rectified by the bridge rectifier (D1–D4) to produce pulsating DC. The pulsating DC is then smoothed by the capacitor (C1) to reduce ripple, and the voltage regulator (U1) provides a stable dc output for the control circuitry. The potentiometer is used to adjust the cutoff voltage. When the battery voltage reaches a set threshold (determined by the potentiometer), the cutoff mechanism will activate. A control circuit, comprising the transistor (Q1), resistors (R1, R2), and capacitor (C3), drives the relay based on the battery's charge state. The relay is connected to the collector of the transistor. The base of the transistor is connected to the potentiometer and through R2 to the battery voltage. Initially, the battery voltage is lower than the threshold set by the potentiometer keeping the transistor ON, energizing the relay coil and allowing current to flow to the battery for charging. When the battery voltage exceeds the threshold set by the potentiometer, the voltage at the transistor's base becomes insufficient to keep it ON and the transistor turns OFF, de-energizing the relay coil. This disconnects the input power from the battery, stopping the charging process to prevent overcharging.

G. *ANSYS Simulation*

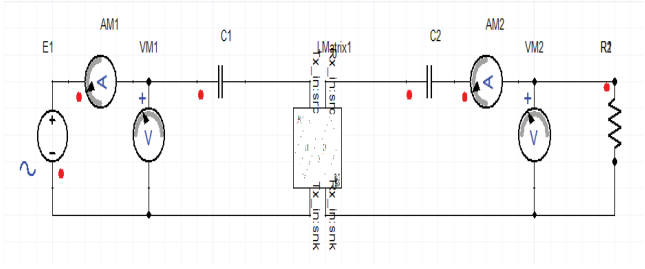

Fig . 6 Circuit Setup in Ansys

Although a completely one-to-one imitation of the desired circuit proved challenging to simulate due to the limitation of the available version of the simulation software Ansys, a miniature model with number of turns 3, diameter 3 cm, diameter of wire 4 mm, pitch of 3 mm and length of the coil 2.1 cm, ultimately having the value of inductance about 100 times smaller than that of the physical coil, was simulated which was a great help in observing and analyzing expected system behavior.

IV. Results

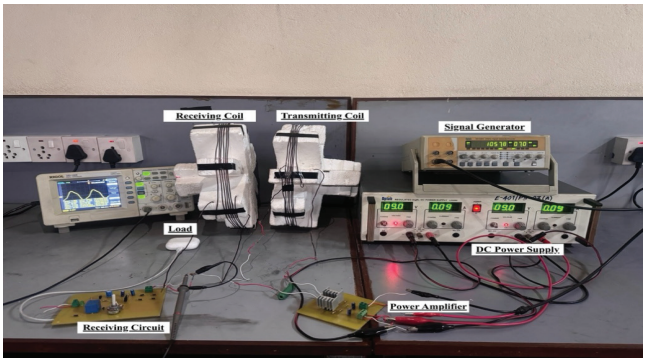

Fig. 7 Proof of Concept Implementation of WPT using MRC

All The experimental validation of the proposed wireless power transfer system was conducted using the testbed, which integrates the signal generation stage, power amplifier module, resonant coil pair, and receiver circuitry. The driving circuit employs a Class B push-pull amplifier topology utilizing TIP41C (NPN) and TIP42C (PNP) bipolar junction transistors. These components were specifically selected for their high collector current capacity (I_C = 6A), enabling the amplifier to sustain the substantial current requirements of the transmitter tank circuit. To manage the thermal dissipation resulting from high-frequency switching at these current levels, aluminum heat sinks were integrated into the PCB design, ensuring junction temperatures remained within safe operating limits during sustained operation.

The optimization of the inductive link required a simultaneous evaluation of inductance and magnetic field intensity. While inductance is fundamental for achieving resonance, the magnetic field intensity (B) governs the effective transmission distance. The magnetic field intensity for a helical coil is defined as:

$$B = \mu_o n I \quad (4)$$

Where n is the number of turns per unit length and I is the current. Conversely, the inductance (L) is determined by the coil's physical dimensions:

$$L = \frac{\mu_o N^2 A}{l} \quad (5)$$

Where N represents the total number of turns and A is the cross-sectional area. The design process involved a critical trade-off between these metrics. For instance, increasing the wire thickness affects the winding density (n); while this may favor inductance, it reduces the number of turns per unit length, thereby diminishing the magnetic field strength and the resultant transmission range.

Furthermore, the coil pitch, the axial distance between adjacent turns significantly influences the system's coupling coefficient. A low pitch increases mutual coupling and concentrates the magnetic field, resulting in higher inductance. However, minimizing the pitch excessively introduces significant parasitic capacitance, which interferes with high-frequency performance and induces unwanted resonance effects. Therefore, the pitch was experimentally tuned to maximize field concentration without compromising resonant stability. Additionally, the coil diameter presented a conflict between energy storage and field distribution. While increasing the diameter expands the cross-sectional area (A) and boosts inductance, it disperses the magnetic flux over a wider region. For this application, a larger diameter was selected specifically to create a dispersed field profile. Although less intense at the center compared to a smaller coil, this broader field distribution is advantageous for wireless charging, as it accommodates imprecise docking alignment between the transmitter and receiver.

These geometric considerations were balanced against the Quality Factor (Q) of the resonant coils. At resonance, where inductive reactance equals capacitive reactance, the Q-factor is inversely proportional to the coil's AC resistance. This resistance is exacerbated by the skin effect, where high-frequency currents are restricted to the conductor's periphery, reducing the effective cross-sectional area. The skin depth decreases as frequency increases according to the relation:

$$\delta = \sqrt{\frac{\rho}{\pi f \mu}} \quad (6)$$

To address these constraints, the final coil geometry was determined through iterative empirical testing. A comparative analysis indicated that a larger coil configuration yielded superior performance by balancing the skin effect, parasitic capacitance, and field distribution. Consequently, the final prototype was constructed using 1.626 mm diameter copper wire wound helically on a Styrofoam form with a 30 cm diameter and 6 turns.

The system performance was validated by empirically tuning the operating frequency to maximize magnetic coupling while mitigating skin-effect losses. As evidenced by the oscilloscope trace in Figure R, a stable sinusoidal waveform was established across the receiver tank, confirming that the resonance condition was successfully achieved. Performance tests demonstrated the system's capability to transfer energy across a significant air gap, successfully delivering 0.5 W of power to the charging load at a transmission distance of 15 cm. The receiver circuit effectively rectified and regulated this induced EMF to charge the test device, confirming the efficacy of the optimized coil geometry in maintaining a high-quality factor while ensuring sufficient magnetic flux density for midrange power transfer.

V. Discussion

A. *Miniature Full System*

As the simulation of a full-scale replica of this project proved impossible, therefore a miniaturized system, with values scaled down as needed, was devised. Following are the results of said miniaturized system.

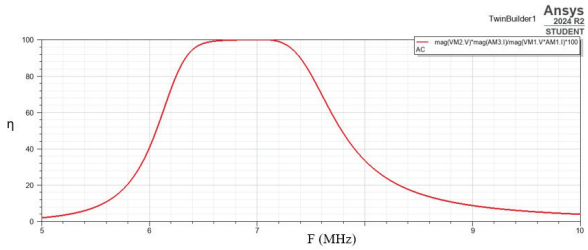

Fig. 8 Variation of efficiency with frequency (ANSYS)

This graph shows the variation of a normalized power transfer parameter with frequency. The curve exhibits a clear resonant behavior, peaking around 1 MHz, indicating that the system operates most efficiently at this frequency. Before 1 MHz, the transfer remains low, and after around 1.028 MHz, it gradually decreases, forming a typical bandpass response. This suggests that the wireless power transfer system is tuned for optimal performance within a narrow frequency range, making it crucial to maintain operation close to this resonance.

B. *Variation of Received Voltage with Coil Orientation*

The magnetic coupling between the helical transmitter and receiver coils is maximum when they are perfectly aligned and facing each other i.e., there is an angle of zero degrees between their centres. Keeping the distance between the coils

constant at around 20 cm and varying the angle between the coils, decrease in the DC voltage across the receiver was observed as the angle between them grew larger, which was expected.

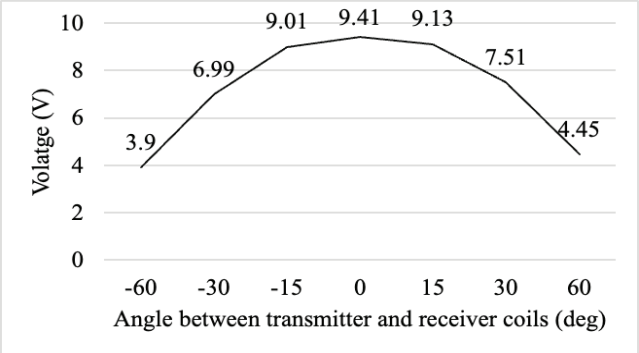

Fig. 9 Variation in Received Voltage with Coil Orientation

C. *Power Vs Distance*

An input RMS voltage of 7V with a current of around 150mA and total DC voltage of 18V with 0.11A of current, i.e., the total power of around 3W is passed to the system of power amplifier and series LC tank. Knowing this and by observing the rectified output DC power in the receiver circuit the end-to-end efficiency of the system was calculated for each distance and depicted in the Fig. 10.

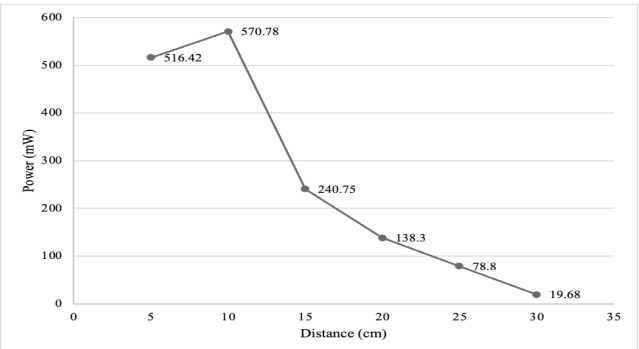

Fig. 10 Variation of Output DC Power with Distance

D. *Comparision between MRC and Inductive Coupling*

As stated, Magnetic resonance coupling utilizes tuned resonant circuits to achieve significantly better efficiency at larger distances compared to standard inductive coupling. This graph of voltage transfer vs. distance between the coils demonstrates the comparatively improved efficiency of magnetic resonant coupling compared to inductive coupling.

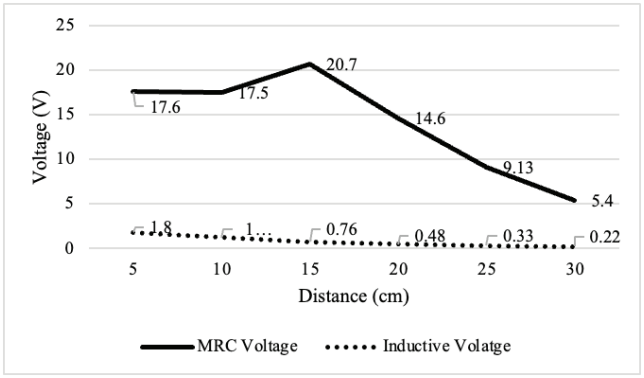

Fig. 11 Comparison between MRC and Inductive Coupling

VI. Conclusions

This paper presents a mid-range wireless power transfer system using magnetic resonance coupling, capable of charging airpods over the distance of around 15 cm. Through empirical analysis, it was verified that the use of magnetic resonance coupling over inductive coupling provides obvious benefits in the form of improved efficiency and increased power-transfer distance. As a proof of concept, implemented with low cost and locally available components, the results indicate that magnetic resonance coupling can be a viable solution for future wireless power applications, paving the way for advancements in charging of consumer electronics, medical devices, and electric vehicles.

Acknowledgement

We, the authors, would like to thank the Department of Electronics and Computer Engineering, Thapathali Campus for providing the opportunity as well as resources (oscilloscope, signal generator, etc) to learn and execute our interest and vision regarding wireless power transfer. We are immensely thankful to our supervisor Er. Kobid Karkee for his mentorship and encouragement throughout the project. We express our gratitude to every involved individual for their valuable support and insightful feedback whose expertise and encouragement have been a great help in shaping the direction and scope of research for this paper. We are also grateful to the authors of various papers that we have referenced for our project as well as the makers of the tools, both software and hardware, used over the course of research and analysis.

References

[1] N. Tesla, "Apparatus for transmitting electrical energy" U.S. Patent 1,119,732, Dec. 1, 1914

[2] J. Garnica, R. A. Chinga, and J. Lin, "Wireless power

transmission: From far field to near field," Proceedings of the IEEE, vol. 101, no. 6, pp. 1321–1331, Jun. 2013, doi: https://doi.org/10.1109/jproc.2013.2251411.

[3] S. Singh, "A research paper on wireless charging," JETIR, vol. 6, no. 5, pp. 50–55, May 2019.

[4] X. Lu, P. Wang, D. Niyato, D. I. Kim, and Z. Han, "Wireless charging technologies: Fundamentals, standards, and network applications," IEEE Communications Surveys & Tutorials, vol. 18, no. 2, pp. 1413–1452, Nov. 2015, doi: https://doi.org/10.1109/comst.2015.2499783.

[5] M. Sharma, M. Solanki, and V. Dave, "Air charging technology," Dogo Rangsang Research Journal, vol. 13, no. 6, pp. 45–52, Jun. 2023.

[6] S. A. Q. Mohammed and J.-W. Jung, "A comprehensive state-of-the-art review of wired/wireless charging technologies for battery electric vehicles: Classification/common topologies/future research issues," IEEE Access, vol. 9, pp. 19572–19585, 2021, doi: https://doi.org/10.1109/access.2021.3055027.

[7] Xiaomi, "Xiaomi Global Home," Xiaomi, 2024. [Online]. Available: https://www.mi.com/global/discover/article?id=1653. [Accessed: Dec. 7, 2024].

[8] M. Z. Aslam, Y. Corre, and Y. Lostanlen, "Effect of human crowd obstruction on the performance of an urban small-cell millimeter-wave access network," in Proc. 2017 IEEE 86th Vehicular Technology Conf. (VTC-Fall), Toronto, ON, Canada, 2017, pp. 1–5, doi: 10.1109/VTCFall.2017.8288371.

[9] Federal Communications Commission, "FCC Rules and Regulations Part 15 Section 247 (15.247)," in "Operation within the bands 902928 MHz, 24002483.5 MHz, and 57255850 MHz," Tech. Rep., 2014.

[10] IEEE Standard for Safety Levels with Respect to Human Exposure to Radio Frequency Electromagnetic Fields, 3 kHz to 300 GHz, IEEE C95.1-2005, pp. 27, Oct. 2005.

[11] H. Basaeri, D. B. Christensen, and S. Roundy, "A review of acoustic power transfer for bio-medical implants," Smart Materials and Structures, vol. 25, no. 12, p. 123001, Nov. 2016, doi: https://doi.org/10.1088/0964-1726/25/12/123001.

[12] Q. Ouyang, G. Xu, K. Liu, and Z. Wang, "Wireless battery charging control for electric vehicles: A user-involved approach," IET Power Electronics, Jun. 2019, doi: https://doi.org/10.1049/iet-pel.2018.6332.

[13] B. Johns, "An introduction to the Wireless Power Consortium standard and TI's compliant solutions," Texas Instruments Incorporated, Power Management, 2011.

[14] M. Al-Saadi, L. Al-Bahrani, M. Al-Qaisi, S. Al-Chlaihawi, and A. Crăciunescu, "Capacitive power transfer for wireless battery charging," Electrotehnica, Electronica, Automatica (EEA), vol. 66, no. 4, pp. 40–51, 2018.

[15] S. Y. Hui, "Planar wireless charging technology for portable electronic products and Qi," Proceedings of the IEEE, vol. 101, no. 6, pp. 1290–1301, Jun. 2013, doi: https://doi.org/10.1109/jproc.2013.2246531.

[16] F. Lu, H. Zhang, and C. Mi, "A review on the recent development of capacitive wireless power transfer technology," Energies, vol. 10, no. 11, p. 1752, Nov. 2017, doi: https://doi.org/10.3390/en10111752.

[17] A. Kurs, A. Karalis, R. Moffatt, J. D. Joannopoulos, P. Fisher, and M. Soljacic, "Wireless power transfer via strongly coupled magnetic resonances," Science, vol. 317, no. 5834, pp. 83–86, Jul. 2007, doi: https://doi.org/10.1126/science.1143254.

[18] M. Dionigi, A. Costanzo, F. Mastri, and M. Mongiardo, "Magnetic resonant wireless power transfer," in Magnetic Resonant Wireless Power Transfer, River Publishers eBooks, 2022, ch. 5, pp. 157–197, doi: 10.1201/9781003340065-5.

[19] D.Wang et al., "Modern Advances in Magnetic Materials of Wireless Power Transfer Systems: A Review and New Perspectives," Nanomaterials, vol. 12, no. 20, p. 3662, Jan. 2022, doi: https://doi.org/10.3390/nano12203662.

[20] Y. Liu and Y. X. Zhang, "Design and analysis of magnetic coupling resonant wireless power transfer system with Class-E inverter," 2017 2nd International Conference on Power and Renewable Energy (ICPRE), Chengdu, China, 2017, pp. 11-14, doi: 10.1109/ICPRE.2017.8390491.

[21] J. Chen, Z. Hu, S. Wang, and Y. Cheng, "Investigation of Wireless Power Transfer for Smart Grid On-line Monitoring Devices under HV Condition," Procedia Computer Science, vol. 83, pp. 1307-1312, 2016.

[22] S. Kuka, K. Ni, and M. Alkahtani, "A Review of Methods and Challenges for Improvement in Efficiency and Distance for Wireless Power Transfer Applications," Power Electronics and Drives, vol. 5, no. 40, pp. 1–25, 2020.

[23] A. Pashaei, E. Aydin, M. A. Özdemir, Y. Kösesoy, and M. T. Aydemir, "A novel hybrid coil design and implementation for wireless power transfer systems," Science and Technology for Energy Transition, vol. 79, pp. 1–9, 2024

[24] I. Khan, M. A. Yar, M. R. Khan, F. Khan, and W. T. Khan, "Bench top wireless power transmission using magnetic resonance for multiple devices," 2017 Progress in Electromagnetics Research Symposium - Fall (PIERS - FALL), pp. 3092–3099, Nov. 2017, doi: https://doi.org/10.1109/piers-fall.2017.8293665.

[25] S. Errede, A Brief History of The Development of Classical Electrodynamics, UIUC Physics 435, Fall Semester 2007, Loomis Laboratory of Physics, Univ. of Illinois at Urbana-Champaign.